Molecular Mechanics Calculations for Aliphatic Ethers Including the Simulations of Infrared and Raman Spectra

Yoshihisa Miwa and Katsunosuke Machida*

Contribution from the Faculty of Pharmaceutical Sciences, Kyoto University, Sakyo-ku, Yoshida, Kyoto 606, Japan. *Received December 16, 1988*

Abstract: The thermodynamic functions and the structures of aliphatic ethers were calculated by using a model force field which includes the atomic charges and charge fluxes as Coulomb potential parameters. These charges and charge fluxes were used also as parameters for the calculation of infrared absorption intensities. The molecular dipole moment vectors of *n*-alkyl ethers were reproduced well by the charge distribution obtained after minimization of energies. The Raman intensities were calculated on the basis of bond polarizability model. The transversal anisotropic components of C–H and C–O bond polarizabilities were introduced to reproduce the molecular polarizability and Raman intensities. The infrared and Raman spectra of *n*-alkyl ethers at room temperature were simulated successfully by using the populations of their rotamers calculated from the free energy differences.

Previously, we proposed a unified method of molecular mechanics calculations and simulations of vibrational spectra by using the atomic charges and charge fluxes as a common set of parameters for the infrared intensities and the intramolecular Coulomb interaction.[1] The newly derived empirical force field was successfully applied to the calculation of free energies and structure parameters of alkanes, and to the simulation of the infrared and Raman spectra of mixtures of rotational isomers of *n*-alkanes at room temperature.[1,2]

In the present work, this approach has been extended to aliphatic ethers. Since the oxygen atom is electronegative and the C–O bond has a large dipole moment, the electrostatic effect may play an important role in determining the energies and structures. In the molecular mechanics calculations published previously on ethers, the electrostatic interaction is described in terms of either the atomic charges[3,4] or the bond dipoles.[5–7] In the MM2 force field,[6] each lone pair of electrons on the oxygen atom is considered as an independent particle like an atomic nucleus involved in various interactions. In the force field we have assumed, the lone pairs on the oxygen atom are not explicitly included to avoid the difficulties associated with the treatment of massless particles in the calculation of vibrational frequencies. The atomic charges were deduced first from the difference in the electronegativities between bonded atoms, and were slightly modified to fit the magnitudes and orientations of the dipole moment vectors of simple *n*-alkyl ethers.[8–11] The charge fluxes were then added in such a way as to reproduce the infrared absorption intensities.

The Raman spectra of *n*-alkyl ethers were simulated by using the bond polarizabilities and their derivatives with respect to internal coordinates as the intensity parameters. On assuming suitable noncylindricity of bond polarizability terms for the C–H and the C–O bonds, tolerable consistency was attained between the anisotropy of molecular polarizability and the Raman band intensities.

Potential Parameters

The potential function adopted in this work is of the same type as used previously for alkanes.[1]

$$V = \sum_i D_i \exp\{-a_i(r_i - r_i^0)\}\,[\exp\{-a_i(r_i - r_i^0)\} - 2] + \sum_i \tfrac{1}{2}H_i(\theta_i - \theta_i^0)^2 + \sum_{ij} F_{ij}(r_i - r_i^0)(r_j - r_j^0) + \sum_{ij} F_{ij}(r_i - r_i^0)(\theta_j - \theta_j^0) + \sum_{ij} F_{ij}(\theta_i - \theta_i^0)(\theta_j - \theta_j^0) + \sum_i V_t(\tau_i) + \sum_{ij} \tfrac{1}{2}V_{Nb}(r_{ij}) + \sum_{ij} \tfrac{1}{2}q_iq_j(1/\epsilon_{ij}r_{ij}) \quad (1)$$

The first five sums of eq 1 represent the energy as a function of the changes of the bond length, r_i, and the valence angles, θ_i. Here, the potential parameters for the internal coordinates not involving the oxygen atom were taken from alkanes[1] without modification. The parameters D_i and r_i^0 in the Morse function for the C–O bond were estimated first from the standard bond energy[12] and the sum of covalent radii,[12] respectively, and a_i was given an arbitrary initial guess, 2.0 Å^{-1}. All the intrinsic valence angles, θ_i, appearing in alkyl ethers were constrained first to be tetrahedral as in the case of alkanes,[1] but that for the angle C–O–C was taken as an adjustable parameter in later calculations. The valence-type force constants related to the oxygen atom were estimated by subtracting the contribution of the last two sums of eq 1 from the corresponding constants of Snyder and Zerbi.[13]

The parameters for the nonbonded O···O interaction in the modified Buckingham-type exchange repulsion–dispersion potential, $V_{Nb}(r_{ij})$, were taken from the crystal structure simulation of oxohydrocarbons by Cox et al.,[14] since these authors used the same parameters for the C···C and the H···H interactions as adopted in our previous work for alkanes.[1] The symmetrical O···O interaction does not appear directly in the present analysis of monoethers, but its parameters are necessary to deduce those for the unsymmetrical atom pairs, O···H and C···O interactions. As in the case of alkanes,[1] the repulsive parameters in the geminal O···O interaction potential were so reduced that the interaction energies deduced for the H···O and the C···O geminal pairs became small enough to give reasonable values of the H–C–O and the C–C–O angles, respectively.

The internal rotation potential around a single bond, $V_t(\tau)$, is written as a truncated Fourier expansion:

$$V_t(\tau) = \tfrac{1}{2}\sum_n V_n\{1 - (-1)^n \cos n\tau\} \quad (2)$$

In the previous work,[1] only the V_3 term was included in the potential for alkanes, and the enthalpy differences among the rotational isomers of *n*-alkanes and the equilibrium structures of cyclic alkanes were fitted simultaneously only by adjusting the nonbonded interaction potentials. Contrarily, the enthalpy dif-

(1) Miwa, Y.; Machida, K. *J. Am. Chem. Soc.* **1988**, *110*, 5183.
(2) Machida, K.; Noma, H.; Miwa, Y. *Indian J. Pure Appl. Phys.* **1988**, *26*, 197.
(3) Bovill, M. J.; Chadwick, D. J.; Sutherland, I. O. *J. Chem. Soc., Perkin Trans. 2* **1980**, 1529.
(4) Wipff, G.; Weiner, P.; Kollman, P. *J. Am. Chem. Soc.* **1982**, *104*, 3249.
(5) Allinger, N. L.; Chung, D. Y. *J. Am. Chem. Soc.* **1976**, *98*, 6798.
(6) Allinger, N. L.; Chang, S. H. M.; Glaser, D. H.; Honig, H. *Isr. J. Chem.* **1980**, *20*, 51.
(7) Burkert, U. *Tetrahedron* **1979**, *35*, 1945.
(8) Blukis, U.; Kasai, P. H.; Myers, R. J. *J. Chem. Phys.* **1963**, *38*, 2753.
(9) Hayashi, M.; Kuwada, K. *Bull. Chem. Soc. Jpn.* **1974**, *47*, 3006.
(10) Hayashi, M.; Kuwada, K. *J. Mol. Struct.* **1975**, *28*, 147.
(11) Kato, H.; Nakagawa, J.; Hayashi, M. *J. Mol. Spectrosc.* **1980**, *80*, 272.
(12) Pauling, L. *The Nature of the Chemical Bond*; Cornell University: Ithaca, NY, 1960.
(13) Snyder, R. G.; Zerbi, G. *Spectrochim. Acta* **1967**, *23A*, 391.
(14) Cox, S. R.; Hsu, L. Y.; Williams, D. E. *Acta Crystallog.* **1981**, *A37*, 293.

0002-7863/89/1511-7733$01.50/0

ferences between the trans and the gauche isomers of methyl ethyl ether and diethyl ether calculated by including only the V_3 term in the C–C–O–C torsional potential is slightly but systematically larger than the observed values.[15-18] According to the ab initio calculation by Radom et al.,[19] the V_1 through the V_3 terms are equally important in the internal rotation potentials of the XCH_2CH_2Y-type molecules. In the present work, the V_2 terms are included in the C–C–O–C and the C–C–C–O torsional potentials in order to reproduce the observed conformational energies and infrared and Raman spectra at room temperature.

The atomic charges in the last sum in eq 1 are expressed as

$$q_i = q_i^0 + \sum_j \frac{\partial q_i}{\partial R_j} R_j \qquad (3)$$

where q_i^0 is the ith intrinsic atomic charge and $\partial q_i/\partial R_j$ is the atomic charge flux with respect to the jth internal coordinate. The initial values of charge fluxes were derived from the infrared intensities as described in the next section. The intrinsic charges were estimated from the electronegativities, χ_i, by

$$q_i^0 = \sum_k^n \beta(\chi_k - \chi_i) \qquad (4)$$

where k runs over the atoms bonded to the ith atom, and β is an adjustable parameter. Each term in the right side of eq 4 corresponds to the effective bond charge defined by van Straten and Smit.[20] Our method is a simplified variation of Del Re's method[21] to calculate the charge distribution of organic molecules under the condition of the electrical neutrality. No limitation is imposed on the value of β in principle, and it may change according to the bond type. For alkanes, however, we need not assume β to be deviated from a narrow range between 0.10 and 0.15. In this work, β was set equal to 0.125 for all the bonds involved in the structure $H–C_\alpha–O–C_\alpha–H$, and the electronegativity of the oxygen atom was slightly modified from the original value[12] of 3.50 to 3.60, in order to reproduce the experimental dipole moment of dimethyl ether[8] (1.31 D). According to the microwave study by Hayashi and Kuwada,[9] the dipole moment of the trans–trans isomer of diethyl ether is about 20% smaller than that of dimethyl ether. These authors attributed the difference in the group moment between methyl and ethyl groups to an induced moment on the C–C bond of the latter.[9] To take account of this effect, we readjusted the atomic charges of the α and the β carbon atoms of each alkoxyl group by transfering a partial charge of 0.032e from α to β. The intrinsic charge of the oxygen atom calculated by this method is −0.275 e and those of the carbon atoms of the α and the β methylene groups are +0.0055 and −0.068 e, respectively.

The potential parameters related to the ether group were refined in two steps, I and II, of interative calculations. Step I is the search for potential minima followed by suitable changes of D_i, r_i^0, θ_i^0, and V_n to improve the calculated thermodynamic data and structures of monoethers containing methyl, ethyl, *n*-propyl, isopropyl, *n*-butyl, and *tert*-butyl groups. Adjustments of q_i^0 under the restriction of eq 4 were occasionally included in this step by taking account of the difference between the calculated and the observed dipole moments. In the beginning of the refinement, a few cycles of step I were carried out to give a stationary set of D_i, r_i^0, θ_i^0, and V_n. Step II is the least-squares fitting of the valence-type force constants through the normal coordinate analysis at the potential minima. The normal equation was constructed from the observed fundamental frequencies of *n*-alkyl monoethers with three to five carbon atoms and the deuteriated derivatives of methyl ethyl ether.[22,23] The Morse parameter a_i was included in this refinement in the form of the stretching constant $2a_i^2D_i$. In later calculations, step II was extended to incorporate simulation of infrared spectra and the subsequent adjustment of the charge fluxes by referring to the L_x matrix elements. Since any changes of the valence-type constants and the charge fluxes gave more or less shifts of potential minima, steps I and II were repeated alternately until an overall convergence was attained. The final values of the parameters newly

Table I. Potential Parameters[a]

Bond Stretching

r_i	a_i, Å^{-1}	D_i, aJ	r_i^0, Å
C1–O	2.146	0.602	1.395
C2–O	2.064	0.617	1.395
C3–O	2.053	0.623	1.395
C4–O	2.039	0.632	1.395

Intrinsic Angle

θ^0_{HCO}	θ^0_{CCO}	θ^0_{COC}
109.47	109.47	101.5

Nonbonded Interaction

r_{ij}	A_{ij},[b] aJ Å	B_{ij},[b] aJ	C_{ij},[c] Å
O···O	1.866	381.98	3.96
O···O (geminal)	1.866	9.65	2.91

Torsion[d]

τ_{ijkl}	V_2, aJ	V_3, aJ	V_6, aJ
H–C–C–O		2.0×10^{-3}	
H–C–O–C		4.0×10^{-3}	
C–C–C–O	-2.0×10^{-3}	2.6×10^{-3}	
C–C–O–C	-3.0×10^{-3}	8.0×10^{-3}	-5.0×10^{-4}

General Quadratic (Diagonal)[e]

symbol	K_{aa}, aJ rad^{-2}	symbol	K_{aa}, aJ rad^{-2}
H_ρ (H–C1–H)	0.520	H_ν, H_Ψ (H–C2–C, H–C3–C)	0.595
H_ϵ (H–C2–H)	0.515	H_σ (H–C1–O)	0.821
H_χ (C–C–O)	1.040	H_μ, H_π (H–C2–O, H–C3–O)	0.885
H_θ (C–O–C)	0.597		

General Quadratic (Off-Diagonal)[e]

symbol	K_{ab}
F_{RS} (C–C, C–O; C common)	0.278
F_S (C–O, C–O; O common)	0.013
$F_{S\mu}$ (C–O, H–C–O; C–O common)	0.432
$F_{R\chi}$ (C–C, C–C–O; C–C common)	−0.082
$F_{S\chi}$ (C–O, C–C–O; C–O common)	0.473
$F_{S\theta}$ (C–O, C–O–C; C–O common)	−0.140
F_μ (H–C–O, H–C–O; C–O common)	0.056
$F_{\epsilon\mu}$ (H–C–H, H–C–O; H–C common)	0.052
$F_{\mu\chi}$ (H–C–O, C–C–O; C–O common)	−0.218
$F_{\mu\nu}$ (H–C–O, H–C–C; H–C common)	0.150
$f^t_{\mu\theta}$, $f^g_{\mu\theta}$ (H–C–O, C–O–C)[f]	−0.050 C_τ
$f^t_{\nu\chi}$, $f^g_{\nu\chi}$ (H–C–C, C–C–O)[f]	−0.076 C_τ
$f^t_{\theta\chi}$, $f^g_{\theta\chi}$ (C–C–O, C–O–C)[f]	−0.113 C_τ
$f^t_{\omega\chi}$, $f^g_{\omega\chi}$ (C–C–C, C–C–O)[f]	−0.090 C_τ

[a] C1, C2, C3, and C4 represent the carbon atoms of CH_3, CH_2, CH, and C groups, respectively. [b] The value for the pair X–Y is the geometric mean of those for the pairs X–X and Y–Y. [c] The value for the pair X–Y is the arithmetic mean of those for the pairs X–X and Y–Y. [d] The value of V_3 for C–C–C–C torsional potential in ref 1 should read 0.918×10^{-3} aJ. [e] The symbols of the force constants in ref 13 are used. The stretch–stretch constants in N cm^{-1}, stretch–bend constants in 10^{-8} N rad^{-1}, and bend–bend constants in aJ rad^{-2}. The same parameters are used for branched alkyl ethers. [f] The dependence on the dihedral angle τ_{ijkl} is introduced by using a factor $C_\tau = \cos \tau_{ijkl}$.

(15) Kitagawa, T.; Miyazawa, T. *Bull. Chem. Soc. Jpn.* **1968**, *41*, 1976.
(16) Perchard, J. P.; Monier, J. C.; Dizabo, P. *Spectrochim. Acta* **1971**, *A27*, 447.
(17) Maissara, M.; Labenne, J. P.; Devaure, J. *J. Chim. Phys.* **1985**, *82*, 451.
(18) Kanesaka, I.; Snyder, R. G.; Strauss, H. L. *J. Chem. Phys.* **1986**, *84*, 395.
(19) Radom, L.; Lathan, W. A.; Hehre, W. J.; Pople, J. A. *J. Am. Chem. Soc.* **1973**, *95*, 693.
(20) van Straten, A. J.; Smit, W. M. A. *J. Mol. Spectrosc.* **1976**, *62*, 297.
(21) Del Re, G. *J. Chem. Soc.* **1958**, 4031.
(22) Shimanouchi, T.; Ogawa, Y.; Ohta, M.; Matsuura, H.; Harada, I. *Bull. Chem. Soc. Jpn.* **1976**, *49*, 2999.
(23) Shimanouchi, T.; Matsuura, H.; Ogawa, Y.; Harada, I. *J. Phys. Chem. Ref. Data* **1978**, *7*, 1323.

Table II. Bond Charge Fluxes[a,b]

Bond Stretching Fluxes, e Å^{-1}			
$\partial q_{CH}/\partial r_{CH}$ (CH_3O)	−0.230	$\partial q_{CO}/\partial r'_{CC}$	−0.350
$\partial q_{OC}/\partial r_{CO}$	0.400	$\partial q_{OC}/\partial r'_{C2O}$ (CH_2OC)	−0.050
Angle Bending Fluxes, e rad^{-1}			
CH_3O Group			
$\partial q_{CH}/\partial\theta_{HCH}$	−0.003	$\partial q_{CH}/\partial\theta_{HCO}$	0.008
$\partial q_{CH}/\partial\theta'_{HCH}$	0.006	$\partial q_{CH}/\partial\theta'_{HCO}$	−0.004
CCH_2O Group[c]			
$\partial q_{CH}/\partial\theta_{HCH}$	−0.005	$\partial q_{CH}/\partial\theta_{HCO}$	0.0025
$\partial q_{CC}/\partial\theta'_{HCH}$	0.002	$\partial q_{CC}/\partial\theta'_{HCO}$	−0.008
$\partial q_{CC}/\partial\theta_{HCC}$	0.008	$\partial q_{CO}/\partial\theta_{HCO}$	−0.005
$\partial q_{CH}/\partial\theta'_{HCC}$	−0.0025	$\partial q_{CH}/\partial\theta'_{CCO}$	0.005
$\partial q_{CO}/\partial\theta'_{HCC}$	0.005	$\partial q_{CC}/\partial\theta_{CCO}$	−0.002
COC Group			
$\partial q_{OC}/\partial\theta_{COC}$	−0.025		

[a] e = electronic unit. [b] The bond charge fluxes for alkyl groups are given in Table II of ref 1, where the first subscript for each q is not given. [c] The parameters for CCH_2O group were commonly used for C_2CHO and C_3CO groups by taking into account redundancy conditions.

introduced for ethers are summarized in Table I. The diminution of the intrinsic C–O–C angle was necessary for compensating the effect of C···C and H···H repulsions between the two alkyl groups attached directly to the oxygen atom.

Spectral Simulation

The infrared spectra were simulated by using the integrated band intensities calculated from the atomic charges at the optimized structure and the atomic charge fluxes (eq 18 in ref 1). To achieve good transferability of parameters among the related local structures, it is useful to express the atomic charge fluxes in terms of the bond charge fluxes.[24,25] For the bond stretching fluxes, this relation is given by

$$\frac{\partial q_i}{\partial R_{ij}} = \frac{\partial q_{ji}}{\partial R_{ij}} - \sum_m \frac{\partial q_{im}}{\partial R_{ij}} \tag{5}$$

Here, $\partial q_{ji}/\partial R_{ij}$ and $\partial q_{im}/\partial R_{ij}$ are the bond charge flux from atom j to atom i and that from atom i to atom m, respectively, associated with the unit increase of the stretching coordinate R_{ij}. The sum in eq 5 is taken over the atoms directly bonded to atom i except atom j, on the assumption that the change of R_{ij} does not give rise to any charge flow along a bond not directly attached to atoms i and j. The total charge is conserved on the change of R_{ij} by virtue of the equation

$$\frac{\partial q_{ji}}{\partial R_{ij}} = -\frac{\partial q_{ij}}{\partial R_{ij}} \tag{6}$$

The charge fluxes around the C–O–C bridge were estimated first from the experimental absolute intensities for dimethyl ether reported by Blom et al.[26] and adjusted a little by referring to the observed infrared spectra on *n*-alkyl ethers in this work. The final values of the bond charge fluxes related to the ether group are shown in Table II. The angle bending fluxes of the H–C–O and the C–C–O coordinates around the α-C atom were mostly determined from the redundancy conditions (eq 21 in ref 1) involving those for the H–C–H and the H–C–C coordinates fixed at the values for alkanes.

The Raman scattering coefficients and the depolarization ratio were calculated from the equilibrium bond polarizabilities and their derivatives with respect to the internal coordinates.[2] Previously, we introduced a noncylindrical polarizability for the C–H bond to reconcile the data of Raman intensities with those of anisotropic molecular polarizabilities of alkanes.[2] In the present work, we have aimed at reproducing the anisotropy of molecular polarizability and the absolute Raman intensities of dimethyl ether simultaneously. This purpose was attained by introducing the transversal anisotropic component in the HCO plane of the C–H bond polarizability, the noncylindrical polarizability for the C–O bond, and the derivative of the latter with respect to the C–O–C bending coordinate. The Raman intensity parameters newly introduced for ethers are listed in Table III. The definitions of the parameters are the same as those in the previous paper[2] except for $\partial\alpha_{ij}/\partial\theta''$ and $\partial\gamma_{ij}/\partial\theta''$, in which the double prime means that the bond ij is attached to a terminal atom of the bending coordinate θ.

Table III. Bond Polarizabilities and Their Derivatives[a]

Equilibrium Parameters[b]			
γ^L_{CH} (CH_3O, CCH_2O)	0.250	α^E_{CH} (CH_3O, CCH_2O)	0.450
$\gamma^T_{CH,O}$ (CH_3O)	0.160	γ^L_{CO}	1.100
$\gamma^T_{CH,O}$ (CCH_2O)	0.080	$\gamma^T_{CO,C}$	−0.280
$\gamma^T_{CH,C}$ (CCH_2O)	0.0375	α^E_{CO}	0.540
Derivatives for Stretching Coordinates[c]			
$\partial\gamma^L_{CH}/\partial r_{CH}$ (CH_3O)	2.600	$\delta\alpha^E_{CO}/\partial r'_{CC}$	0.300
$\partial\gamma^L_{CH}/\partial_{CH}$ (CCH_2O)	1.980	$\partial\gamma^L_{CO}/\partial r_{CO}$	1.000
$\partial\alpha^E_{CH}/\partial r_{CH}$ (CH_3O)	0.680	$\partial\alpha^E_{CO}/\partial r_{CO}$	0.800
$\partial\alpha^E_{CH}/\partial r_{CH}$ (CCH_2O)	0.450	$\partial\alpha^E_{CH}/\partial r'_{CO}$	−0.150[d]
$\partial\gamma^L_{CO}/\partial r'_{CC}$	−0.200	$\partial\alpha^E_{CO}/\partial r'_{CO}$	−0.550[d]
$\partial\gamma^L_{CO}/\partial r'_{CC}$ (CH_3CH_2O)	−0.350		
Derivatives for Bending Coordinates[e]			
CH_3O Group			
$\partial\alpha^E_{CH}/\partial\theta^i_{HCO}$	0.200	$\partial\alpha^E_{CO}/\partial\theta^{i'}_{HCH}$[f]	−0.050
$\partial\alpha^E_{CH}/\partial\theta^{0'}_{HCO}$	−0.100	$\partial\gamma^L_{CH}/\partial\theta_{HCH}$	−0.200
$\partial\gamma^L_{CO}/\partial\theta^i_{HCO}$	−0.200	$\partial\gamma^L_{CH}/\partial\theta'_{HCH}$	0.400
$\partial\gamma^L_{CO}/\partial\theta^0_{HCO}$	0.100	$\partial\gamma^L_{CH}/\partial\theta_{HCO}$	−0.100
$\partial\alpha^E_{CO}/\partial\theta^i_{HCO}$	0.050	$\partial\gamma^L_{CH}/\partial\theta^i_{HCO}$	0.050
CCH_2O Group			
$\partial\gamma^L_{CH}/\partial\theta_{HCC}$	−0.350	$\partial\gamma^L_{CO}/\partial\theta''_{HCC}$	0.050
$\partial\gamma^L_{CH}/\partial\theta'_{HCC}$	0.350	$\partial\gamma^L_{CO}/\partial\theta''_{CCC}$	−0.100
$\partial\gamma^L_{CO}/\partial\theta'_{HCC}$	0.100	$\partial\alpha^E_{CO}/\partial\theta''_{HCC}$	0.125
$\partial\gamma^L_{CO}/\partial\theta_{HCO}$	−0.150	$\partial\alpha^E_{CO}/\partial\theta''_{CCC}$	−0.250
$\partial\gamma^L_{CO}/\partial\theta_{CCO}$	0.100	$\partial\gamma^L_{CC}/\partial\theta''_{COC}$	0.100
$\partial\alpha^E_{CH}/\partial\theta_{HCH}$	−0.075	$\partial\alpha^E_{CC}/\partial\theta''_{COC}$	0.100
$\partial\alpha^E_{CH}/\partial\theta'_{CCO}$	0.075		
COC Group			
$\partial\gamma^L_{CO}/\partial\theta_{COC}$	−0.050	$\partial\alpha^E_{CO}/\partial\theta_{COC}$	0.080
$\partial\gamma^T_{CO,C}/\partial\theta_{COC}$	0.250		

[a] The meanings of the symbols are the same as those in the previous work.[2] [b] In Å^3. [c] In Å^2. [d] The parameter for dimethyl ether was set equal to zero. [e] In Å^3 rad^{-1}. [f] θ^i_{HCH} is the H–C–H angle opposite to θ^i_{HCO}.

The infrared and Raman spectra of *n*-alkyl ethers at room temperature were simulated by superposing the calculated spectra of the rotamers with the populations derived from the calculated thermodynamic functions according to the procedure described previously.[1,2] The branched alkyl ethers are not included in the spectral simulation because the valence-type force constants related to the secondary through quaternary carbon atoms have not been refined satisfactorily in our force field.

Results and Discussion

The calculated heats of formation and molar entropies of simple aliphatic ethers are compared with the experimental values in Table IV. To reproduce the differences in the heats of formation among the structural isomers, it was necessary to adjust the values of D_i for the C–O bonds separately for primary, secondary, and tertiary alkoxyl groups. The increments of these values are of the same magnitude as those for the C–C bond in the case of alkanes.[1] For *n*-alkyl ethers, the fully extended forms are not necessarily the major component of rotamers at room temperature. Nevertheless, corrections for the coexistence of different isomers to the heats of formation and entropies are negligible (less than 1.0%) because of the Boltzmann factor. Thus, only the values for the fully extended isomers are shown in Table IV. The thermodynamic quantities of branched alkyl ethers were calculated by using the valence force constants and the charge fluxes refined

(24) Decius, J. C. *J. Mol. Spectrosc.* **1975**, *57*, 348.
(25) Gussoni, M. *J. Mol. Struct.* **1984**, *113*, 323.
(26) Blom, C. E.; Altona, C.; Oskam, A. *Mol. Phys.* **1977**, *34*, 557.

Table IV. Heats of Formation and Molar Entropies

molecule	ΔH_f[a] exptl[c]	ΔH_f[a] calcd	S[b] exptl[d]	S[b] calcd
dimethyl ether	−184.1 ± 0.5	−181.5	267	264
methyl ethyl ether	−216.4 ± 0.7	−217.6	310	301
diethyl ether	−252.1 ± 0.8	−253.5	343	327
methyl *n*-propyl ether	−238.2 ± 0.7	−237.7	350	333
methyl isopropyl ether	−252.0 ± 1.0	−250.6	339	329
methyl *tert*-butyl ether	−283.5 ± 1.1	−283.3	353	342
di-*n*-propyl ether	−292.9 ± 1.1	−293.8	423	391
diisopropyl ether	−319.2 ± 1.6	−319.9	390	380
di-*n*-butyl ether	−333.4 ± 1.4	−330.9	501	455

[a] In kJ mol^{-1}. [b] In J deg^{-1} mol^{-1}. [c] Pedley, J. B.; Naylor, R. D.; Kirby, S. P. *Thermochemical Data of Organic Compounds*, 2nd ed.; Chapman and Hall: London, 1986. [d] Stull, D. R.; Westrum, E. F., Jr.; Sinke, G. C. *The Chemical Thermodynamics of Organic Compounds*; Wiley: New York, 1969.

Table V. Thermodynamic Functions of Rotamers of Aliphatic Ethers

molecule		ΔH[a]	ΔS[b]	ΔG[a]	population
diethyl ether	TT				0.729
	TG	6.15	6.04	4.35	0.252
	GG	11.60	2.77	10.77	0.019
methyl *n*-propyl ether	TT				0.280
	TG	−0.58	−1.03	−0.27	0.626
	GT	6.60	−0.42	6.72	0.037
	GG	5.22	−1.64	5.70	0.057
ethyl *n*-propyl ether	TTT				0.243
	TTG	−0.66	−0.98	−0.37	0.562
	TGT	6.57	−0.31	6.66	0.033
	GTT	6.10	3.06	5.18	0.060
	TGG	4.83	−1.30	5.21	0.059
	GTG	5.13	−2.98	6.02	0.043
methyl *n*-butyl ether	TTT				0.163
	TTG	2.20	−0.95	2.48	0.120
	TGT	−0.89	−1.18	−0.54	0.405
	GTT	6.36	2.70	5.55	0.035
	TGG	1.35	−1.51	1.78	0.158
	TGG′	3.43	−1.15	3.77	0.071
	GGT	4.55	−0.73	4.77	0.048

[a] In kJ mol^{-1}. [b] In J deg^{-1} mol^{-1}.

for *n*-alkyl ethers. Fitting of these parameters to the vibrational data of branched ethers may bring about certain deviations of the calculated heats of formation within the experimental uncertainties. In analogy with the case of alkanes, the observed heats of formation of branched alkyl ethers are appreciably smaller than those of the corresponding *n*-alkyl ethers. The effect of branching for ethers is more conspicuous than for alkanes.[1] The enthalpy difference between primary and secondary alkyl ethers is about 14 kJ mol^{-1} per one secondary alkyl group, while the corresponding difference for alkanes is about 8 kJ mol^{-1}. In the present calculation, the Coulomb attraction between each hydrogen atom and the carbon or the oxygen atom at its vicinal position plays an essential role in stabilizing branched alkyl ethers. The molar entropies were derived from the calculated values of the principal moments of inertia and the normal frequencies.[27] The agreement between the calculated and the experimental entropies is satisfactory for small ethers, but systematic deviations arise in larger derivatives from the underestimation of the torsional contribution due to the harmonic approximation.

The rotational barrier for the *O*-methyl group calculated from the present potential, 10.4 kJ mol^{-1}, agrees well with the experimental value of 10.7 kJ mol^{-1}.[10,28] The differences in enthalpies and entropies among rotational isomers of *n*-alkyl ethers and their populations at room temperature are shown in Table V. The enthalpy difference between the gauche and the trans conformers of methyl ethyl ether was so adjusted as to reproduce the experimental value in the gaseous state[15] by incorporating the negative V_2 term into the torsional potential. The enthalpy difference between the trans–trans and the trans–gauche conformers of diethyl ether calculated by using this V_2 term is close to the experimental values estimated from the infrared spectra, 5.73 kJ mol^{-1},[16] and the Raman spectra, 5.9 or 6.5 kJ mol^{-1},[17] in the liquid state, but higher than the recent value estimated from the Raman spectra in the gaseous state, 4.8 kJ mol^{-1}.[18]

The calculated structure parameters are compared with the experimental values in Table VI. The calculated variations in the C–O bond length and the C–O–C angle on the alkyl branching at the α position follow the observed trend[29,30] quite well. According to the results of the electron diffraction measurement of methyl *tert*-butyl ether,[29] the angle spanned between the symmetry axes of methyl and *tert*-butyl groups is larger than the C–O–C angle. This trend of the tilts of the terminal groups is also reproduced well by the present force field. A trial calculation without introducing the charge fluxes into the force field failed

Table VI. Structure Parameters[a]

molecule	parameter	exptl[b]	calcd	ref
dimethyl ether	r(C–O)	1.415 (1)	1.411	*c*
	∠COC	111.8 (2)	112.7	
	δ_{ME}[d]	3.6 (17)	2.0	
methyl ethyl ether	$r(CH_3–O)$	1.413 (9)	1.414	*e*
	$r(CH_2–O)$	1.422 (7)	1.419	
	r(C–C)	1.520 (4)	1.529	
	∠COC	111.9 (5)	112.6	
	∠CCO	109.4 (4)	108.1	
	θ_g[f]	84 (6)	80.4	
diethyl ether	r(C–O)	1.411 (3)	1.423	*g*
	r(C–C)	1.517 (5)	1.524	
	∠COC	112.1 (3)	112.6	
	∠CCO	108.4 (3)	107.9	
methyl *tert*-butyl ether[j]	$r(C_2–O)$	1.448 (4)	1.446	*h*
	$r(C_6–O)$	1.415	1.427	
	r(C–C)	1.532 (2)	1.530	
	∠COC	118.9 (14)	119.2	
	∠CCC	111.1 (2)	109.9	
	ϕ_4	13 (4)	10.4	
	δ	4.6 (6)	5.4	
	δ_6	1	2.6	
diisopropyl ether[k]	r(C–O)	1.431 (3)	1.439	*i*
	r(C–C)	1.526 (3)	1.520	
	∠COC	118.5 (16)	117.0	
	$\angle OCC_3$	110.3 (4)	110.8	
	$\angle OCC_4$	106.5 (6)	106.5	
	∠CCC	113.5 (11)	111.3	
	ϕ_1	39 (4)	38.6	
	$\tau(C_5OC_2C_3)$	−80	−83.1	
	$\tau(C_5OC_2C_4)$	156	155.7	

[a] Distances in Å; angles in deg. [b] Values in parentheses are the limits of error attached to the last digit of the parameter values. [c] Tamagawa, K.; Takemura, M.; Konaka, S.; Kimura, M. *J. Mol. Struct.* **1984**, *125*, 131. [d] The tilt angle of the methyl groups. [e] Oyanagi, K.; Kuchitsu, K. *Bull. Chem. Soc. Jpn.* **1978**, *51*, 2237. [f] The dihedral angle for the gauche conformaer. [g] Hayashi, M.; Adachi, M.; *J. Mol. Struct.* **1982**, *78*, 53. [h] Reference 29. [i] Reference 30. [j] For symbols, see ref 29. [k] $\tau(C_lOC_mC_n)$ means the dihedral angle $C_lOC_mC_n$. For the other symbols, see ref 30.

Table VII. Molecular Dipole Moments[a]

molecule	exptl[b]	calcd
dimethyl ether	1.31 ± 0.01[c]	1.304
diethyl ether	1.061 ± 0.018[d]	1.092
methyl ethyl ether	1.174 (22)[e]	1.200
methyl *n*-propyl ether	1.107 (13)[f]	1.100
methyl isopropyl ether	1.247 (8)[g]	1.238

[a] In debye. [b] Error estimates in the original works are given. [c] Reference 8. [d] Reference 9. [e] Reference 10. [f] Reference 11. [g] Nakagawa, J.; Imachi, M.; Hayashi, M. *J. Mol. Struct.* **1984**, *112*, 201.

(27) Rossini, F. D. *Chemical Thermodynamics*; Wiley: New York, 1950. Pitzer, K. S.; Gwinn, W. D. *J. Chem. Phys.* **1942**, *10*, 428.
(28) Kitagawa, T.; Ohno, K.; Sugeta, H.; Miyazawa, T. *Bull. Chem. Soc. Jpn.* **1972**, *45*, 969.
(29) Suwa, A.; Ohta, H.; Konaka, S. *J. Mol. Struct.* **1988**, *172*, 275.
(30) Takeuchi, H.; Fujii, M.; Konaka, S.; Kimura, M. *J. Phys. Chem.* **1987**, *91*, 1015.

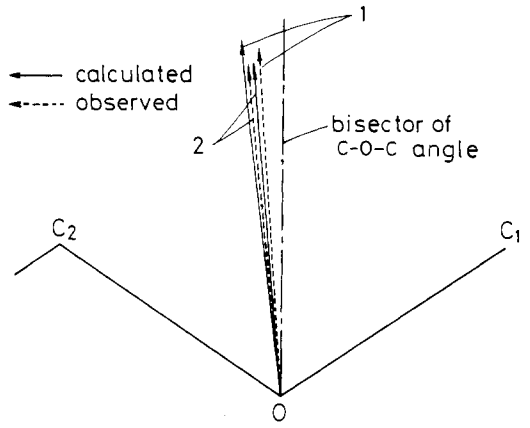

Figure 1. Molecular dipole moment vectors of methyl ethyl ether (1) and methyl *n*-propyl ether (2). C_1 and C_2 represent methyl and methylene carbons, respectively.

to reproduce the observed difference between the two C–O bond lengths of *tert*-butyl methyl ether.

The molecular dipole moments calculated from the present charge distribution and the optimized structures are compared with the experimental values in Table VII. In earlier studies on the molecular mechanics calculations for ethers,[3,5,6] the atomic charges or the bond dipole moments were estimated almost exclusively from the observed dipole moment of dimethyl ether. Dipole moments of higher alkyl ethers and their orientation relative to the molecular axes have not fully been referred to. In this work, the observed difference between the dipole moments of dimethyl ether[8] and diethyl ether[9] is reproduced well by the aforementioned transfer of charges through the C–C bond directly adjoining the oxygen atom. The dipole moment vectors of *n*-alkyl methyl ethers derived from the atomic charges for the equilibrium structure are shown in Figure 1 together with those determined by the microwave spectra.[10,11] The calculated difference in magnitudes of the dipole moments between methyl ethyl ether and methyl *n*-propyl ether is consistent with the experimental values.[10,11] The agreement is due mainly to the difference between the intrinsic hydrogenic charge on the *C*-methyl group, 0.04 e, and that on the *O*-methyl group, 0.05 e, in the charge distribution adopted in this work. The tilts of the calculated dipole moments from the bisector of the C–O–C angle are in the correct direction, but their magnitudes change with the *n*-alkyl length in a way reverse to the experiment. To discuss the problem in more detail, however, the experimental results for larger ethers are required at least to reveal the influence of the even–odd alternation of *n*-alkyl carbon atoms.

The normal frequencies calculated from the present force field are a little less accurate than those derived from the well-known force fields adapted for normal coordinate analyses.[13,22,23] The standard deviation below 1500 cm^{-1} for *n*-alkyl monoethers with three to five carbon atoms and the deuteriated derivatives of methyl ethyl ether is 13.5 cm^{-1}, while the deviation in the local symmetry force field[23] is 6.2 cm^{-1} and the deviation for methyl ethyl ether and diethyl ether in the force field[13] of Snyder and Zerbi is 9.5 cm^{-1}.

The absolute infrared absorption intensities of dimethyl ether were calculated from the charges given by eq 3 at the energy minima and the charge fluxes in Table II. They agree well with the experimental values in the gas phase[26] as shown in Table VIII. The observed C–H stretching intensity of dimethyl ether is greater than that of ethane (178 km mol^{-1}).[31] The excess intensity for ethers was interpreted by Castiglioni et al.[32] as due to enrichment of the electronic charge of hydrogen atoms in the C–H bonds at the trans position with respect to the oxygen lone pairs. In this work, the hydrogenic charges were assumed to be independent of the orientation of the C–H bond to simplify the automatic specification of relevant atoms in the computer program. The

(31) Kondo, S.; Saeki, S. *Spectrochim. Acta* **1973**, *29A*, 735.
(32) Castiglioni, C.; Gussoni, M.; Zerbi, G. *J. Mol. Struct.* **1986**, *141*, 341.

Table VIII. Infrared Intensities, Molecular Polarizability, Raman Intensities, and Depolarization Ratio of Dimethyl Ether

Infrared Intensities

ν, cm^{-1}		Ai (10^6 cm mol^{-1})	
exptl	calcd	exptl[a]	calcd
2999-2820	2987~2868	25.3	24.5
1485~1432	1462~1427	2.2	2.4
1250~1179	1230~1194	8.8	8.3
1104	1057	3.9	5.6
931	924	2.6	2.8
424	429	0.4	0.4

Molecular Polarizability[b]

	exptl		calcd
α_{xx}	6.38[c]	6.02[d]	6.03
α_{yy}	4.39	4.82	4.51
α_{zz}	4.94	4.82	4.85

Raman Intensities and Depolarization Ratio

ν, cm^{-1}		S^e		ρ	
exptl	calcd	exptl[e]	calcd	exptl	calcd
2999~2820	2987~2868	13.4	13.4	0.17	0.23
1485~1432	1462~1427	1.0	1.0	0.67	0.65
1250~1104	1230~1057	0.23	0.63	0.75	0.62
931	924	0.61	0.65	0.25	0.02
424	429	0.08	0.06	0.14	0.13

[a] Reference 26. [b] In Å^3. [c] Quoted by: Applequist, J.; Carl, J. R.; Fung, K. K. *J. Am. Chem. Soc.* **1972**, *94*, 2952. [d] Bogaard, M. P.; Buckingham, A. D.; Pierens, R. K.; White, A. H. *J. Chem. Soc., Faraday Trans. 1* **1978**, *74*, 3008. [e] Reference 26. The intensities relative to the sum of the fundamentals, ν_3, ν_4, ν_{10}, ν_{11}, ν_{15}, and ν_{19}.

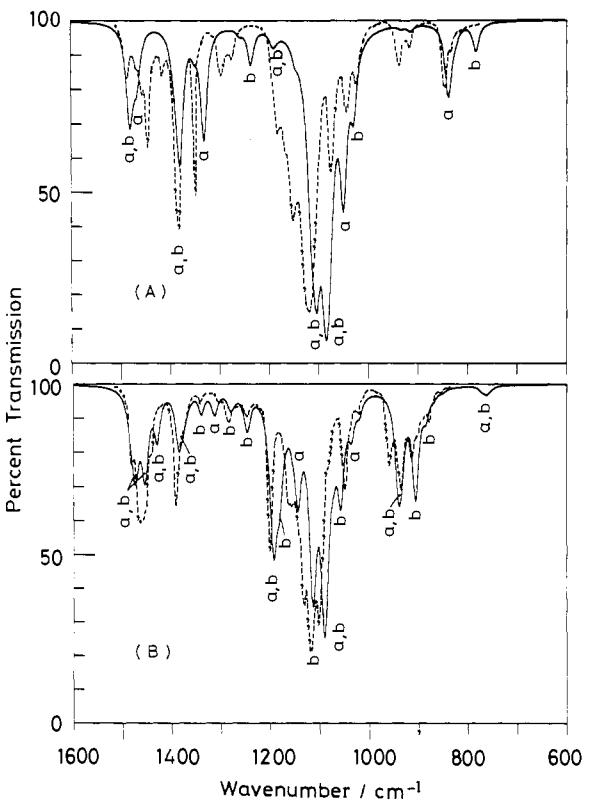

Figure 2. Simulated (solid line) and observed (broken line) infrared spectra of diethyl ether (A) and methyl *n*-propyl ether (B). The symbols a and b represent the conformers TT and TG, respectively (T = trans and G = gauche[22]). The spectra were measured with a JASCO IRA-2 IR spectrometer: slit width 1.5 cm^{-1} at 1000 cm^{-1}; path length 0.1 mm; CCl_4 solution. The concentrations of diethyl ether and methyl *n*-propyl ether were 0.55 and 0.60 mol dm^{-3}, respectively.

C–H stretching intensity of dimethyl ether was reproduced by slightly modifying the flux parameter, $\partial q_{CH}/\partial r_{CH}$, from 0.216 e

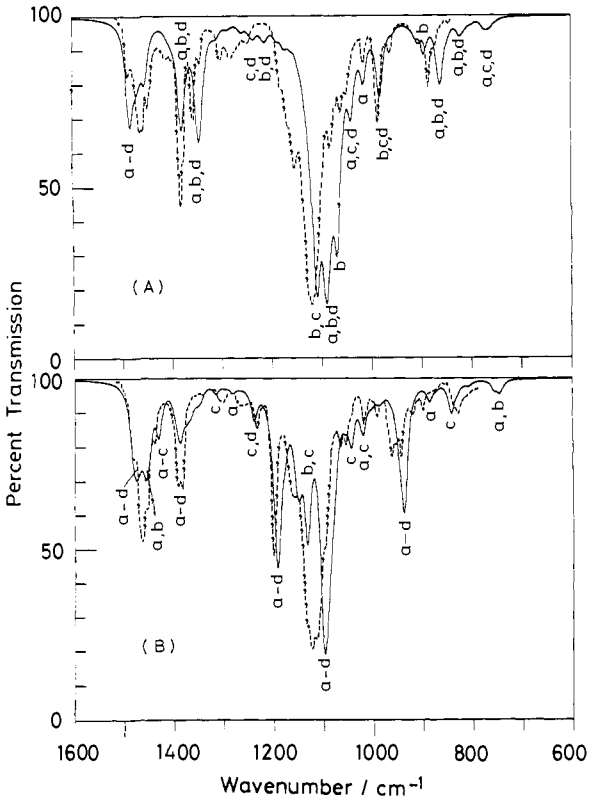

Figure 3. Simulated (solid line) and observed (broken line) infrared spectra of ethyl *n*-propyl ether (A) and methyl *n*-butyl ether (B). The symbols a, b, and d represent TTT, TTG, and TGG,[22] respectively. The symbol c represents GTT for ethyl *n*-propyl ether and TGT for methyl *n*-butyl ether,[22] respectively. The concentrations of ethyl *n*-propyl ether and methyl *n*-butyl ether were 0.54 and 0.58 mol dm^{-3}, respectively. For the other experimental conditions, see caption of Figure 2.

Å^{-1} for *n*-alkanes to 0.230 e Å^{-1}.

In Figures 2 and 3, the simulated infrared absorption spectra of *n*-alkyl ethers with four to five carbon atoms at 25 °C are compared with the spectra observed in the CCl_4 solutions. It has long been recognized that the band intensities measured in condensed phases must be corrected for the effect of the internal electric field, and several equations have been proposed for the use in such a correction.[33-38] According to the Polo–Wilson equation,[33] which has been widely used for pure liquids and solutions,[34,35] the intensities in a dilute solution with a refractive index of about 1.40 are calculated to be about 30% greater than those in the gas phase. Contrarily, a new equation recently proposed by Akiyama[37,38] predicts that the intensities in this solution are almost the same as, or slightly less than, the gas-phase values. In the present study, the spectra were simulated by using the intensity parameters estimated from the experimental absolute intensities in the gas phase and were not corrected for the change of states. The half-bandwidth was assumed to be 15 cm^{-1} by comparing the peak transmittance and the bandwidth of the C–O stretching band near 1100 cm^{-1} with those of the observed spectra. Agreement between the simulated and the calculated spectra is generally good as shown in Figures 2 and 3. We cannot decide, however, whether the internal field effect is really negligible for ethers, since the intermolecular interactions in the liquid phase often give rise to appreciable changes of infrared intensities.[39,40]

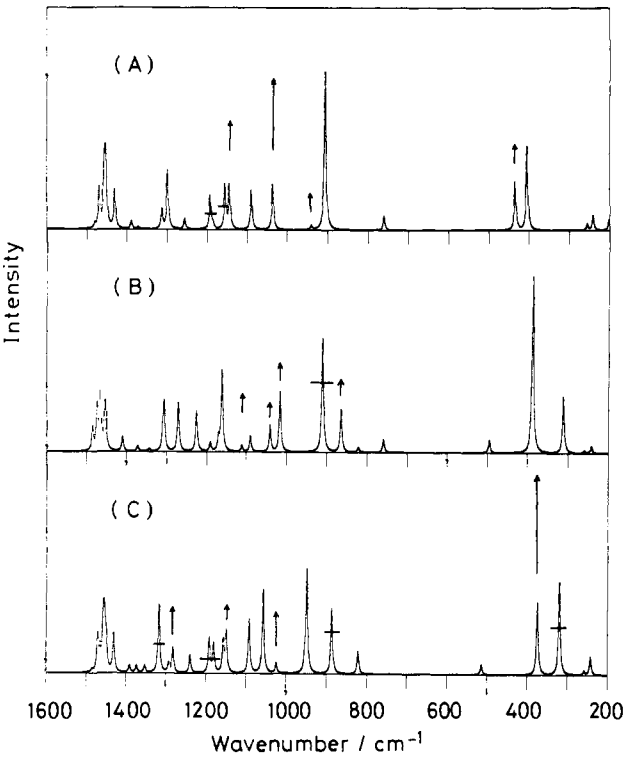

Figure 4. Simulated Raman spectra of methyl *n*-propyl ether (A), ethyl *n*-propyl ether (B), and methyl *n*-butyl ether (C) in all-trans form. The half-bandwidth (ω) is assumed to be 5.0 cm^{-1}.

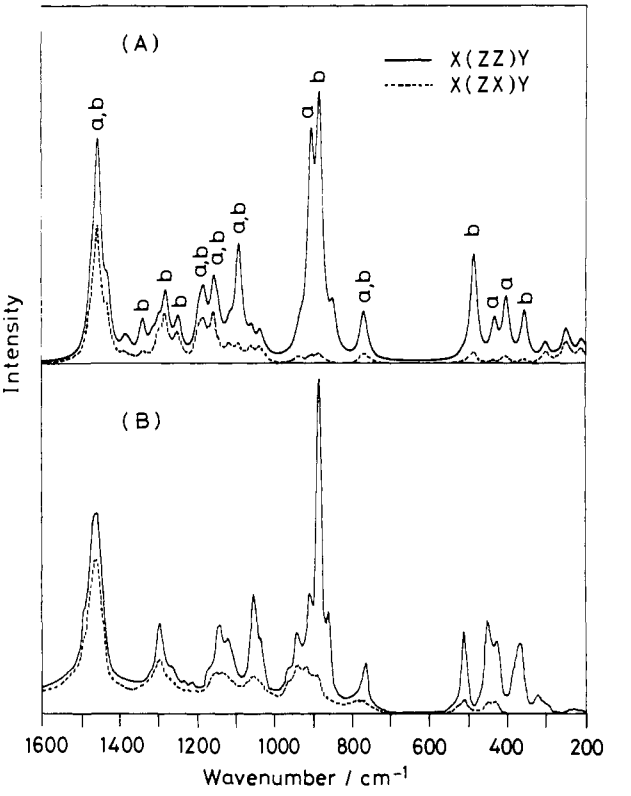

Figure 5. Polarized Raman spectra of liquid methyl *n*-propyl ether at room temperature: (A) simulated, ω = 20 cm^{-1}; (B) observed, recorded on a JEOL S-1 laser Raman spectrophotometer, excited at 514.5 nm by a NEC GLG 3200 Ar^+ laser (120 mW at the sample position); slit width, 12 cm^{-1} at 1000 cm^{-1}. For the symbols a and b, see caption of Figure 2.

The conformers contributing to the band intensities are indicated for main peaks in the calculated spectra in Figures 2 and 3. The band assignments to individual rotamers and their vibrational

(33) Polo, S. R.; Wilson, M. K. *J. Chem. Phys.* **1955**, *23*, 2376.
(34) Mallard, W. C.; Straley, J. W. *J. Chem. Phys.* **1957**, *27*, 877.
(35) Person, W. B. *J. Chem. Phys.* **1958**, *28*, 319.
(36) Clifford, A. A.; Crawford, B., Jr. *J. Phys. Chem.* **1966**, *70*, 1536.
(37) Akiyama, M. *J. Chem. Phys.* **1984**, *81*, 5229.
(38) Akiyama, M. *J. Chem. Phys.* **1986**, *85*, 7.
(39) Mulliken, R. S.; Person, W. B. *Molecular Complexes*; Wiley: New York, 1969.
(40) Kakimoto, M.; Fujiyama, T. *Bull. Chem. Soc. Jpn.* **1975**, *48*, 2258.

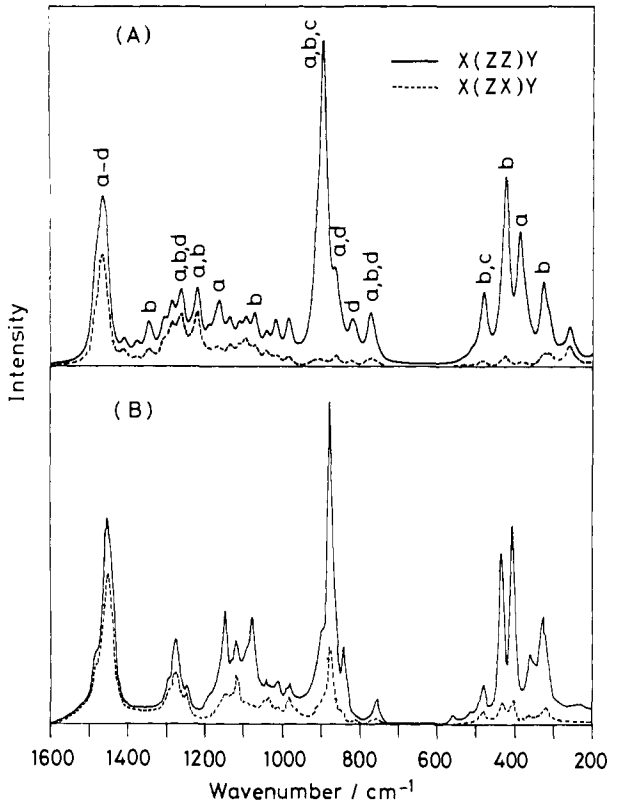

Figure 6. Polarized Raman spectra of liquid ethyl *n*-propyl ether at room temperature: (A) simulated, (B) observed. For the symbols a–d and for the experimental conditions, see captions of Figures 3 and 5, respectively.

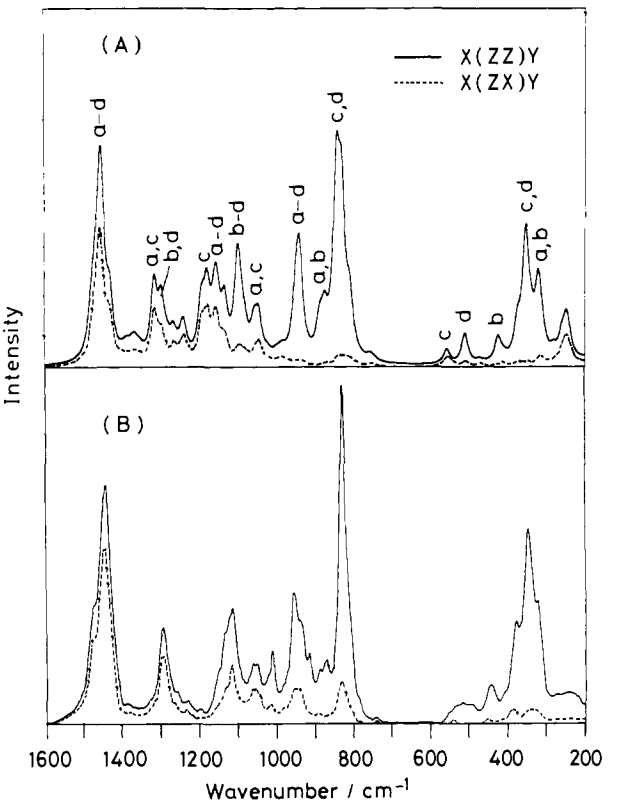

Figure 7. Polarized Raman spectra of liquid methyl *n*-butyl ether at room temperature: (A) simulated, (B) observed. For the symbols a–d and for the experimental conditions, see captions of Figures 3 and 5, respectively.

modes agree well with those given by Shimanouchi, et al.[23]

The calculated values of molecular polarizability components, Raman band intensities, and depolarization ratios of dimethyl ether are compared with the experimental values in Table VIII. To reproduce as large an anisotropy of the molecular polarizability as noticed in the difference between α_{xx} and α_{yy}, we should attribute a large anisotropic component, γ^{L}_{CO}, to the C–O bond polarizability. The increase of γ^{L}_{CO}, however, results in an unreasonable enhancement of the Raman intensities of the normal modes involving the bending motion of the C–O–C bridge calculated at 1230 and 429 cm^{-1}. The effect of large γ^{L}_{CO} is partly suppressible by introducing an appreciable transversal anisotropy to the C–H bond polarizability, $\gamma^{T}_{CH,O}$, as for alkanes in the previous work.[2] Adjustment of $\partial\gamma^{L}_{CO}/\partial\theta_{COC}$ and $\partial\gamma^{T}_{CO,C}/\partial\theta_{CO}$ were also found effective to reduce the extra intensities of the calculated modes at 1230 and 429 cm^{-1}.

The simulated Raman spectra of the extended forms of methyl *n*-propyl ether, ethyl *n*-propyl ether, and methyl *n*-butyl ether are shown in Figure 4, where the vertical arrows and the horizontal lines indicate, as for the previously reported *n*-alkanes,[2] the relative intensities in the observed spectra in the solid state.[22] The large γ^{L}_{CO} mentioned above also gives rise to an unreasonable increase of the intensities of the bands near 250 cm^{-1} due to torsional modes involving the rotation of a C–O bond around the neighboring bonds. Such an intensity increase can be reduced by introducing a negative $\gamma^{T}_{CO,C}$, which means that the C–O bond polarizability extends out of the COC plane. The band intensities near 400 cm^{-1} of methyl *n*-propyl ether and ethyl *n*-propyl ether were adjusted by introducing the new types of parameters, $\partial\gamma^{L}_{CO}/\partial\theta''_{CCC}$, $\partial\alpha^{E}_{CO}/\partial\theta''_{CCC}$, $\partial\gamma^{L}_{CC}/\partial\theta''_{COC}$, and $\partial\alpha^{E}_{CC}/\partial\theta''_{COC}$. The peak heights of some bands in the region 1000–1200 cm^{-1} arising from the C–C stretching and the methyl rocking modes of the alkyl chains are not well reproduced. Some of these discrepancies may be due to the constraint of the homogeneous half-bandwidth. Detailed experimental data for the absolute intensities of these bands of alkanes and ethers are required to modify the parameters for further fitting of these band intensities.

In Figures 5–7, the polarized Raman spectra of the same ethers as shown in Figure 4 are simulated at 25 °C and are compared with the observed spectra in the liquid state at room temperature. The bands in the region 1000–1400 cm^{-1} of the simulated spectra are scattered more widely than in the observed spectra, giving rise to many extra peaks. The band intensities contributed from the gauche conformers in the region 300–500 cm^{-1} are a little larger than those in the observed spectra. On the other hand, the appearance of many bands assignable to different rotamers on increasing the temperature and the patterns of the strong bands in the region 800–1000 cm^{-1} are reproduced well with the population obtained from the present potential. The simulation was also successful in reproducing the large depolarization ratio of the strong band near 1450 cm^{-1} in the observed spectra. Extension of the present calculation to diethers is now in progress.

Acknowledgment. We thank Takahide Fukuda for his technical assistance. This work was supported by a Grant-in-Aid for Scientific Research (No. 62570964) from the Ministry of Education, Science, and Culture. The calculation in this work was performed on FACOM M-780 and FACOM VP-200 computer systems in the Data Processing Center, Kyoto University.